USA) and MyosinVIIa (1:500; Proteus Bio Sciences, CA, USA). Secondary antibodies used were Alexa-Fluor donkey anti-rabbit (1:500; Molecular Probes, Eugene, OR, USA). Images of sections were captured on a Zeiss Axioplan2 microscope using an AxioCam HRc CCD camera and Axio Vision Rel.4.2 software.

Quantification and statistical analysis

The number of microtubules of the IPC in 50 fields randomly selected was counted at magnifications of ×10,000, and was compared between R75W+ and non-Tg mice. The results were expressed as mean±S.D. Statistical significance was addressed by Student's *t*-test; $P<0.05$ was accepted as significant.

For measurement of the height and the cells area of the organ of Corti, midmodiolar section (1 μm) were counterstained with Toluidine Blue as described (Faddis et al., 1998). Digital light micrograph images of the organ of Corti were captured using following software. The height and the cell area of the organ of Corti were measured by using NIS Elements-D (Nikon, Tokyo, Japan). Two animals from each age group were analyzed.

RESULTS

The different findings were observed by ABR measurements in a group of R75W+ and non-Tg mice at the stage of hearing development (Fig. 1). The onset of hearing in non-Tg mice was recognized at P11 as previously described (Anniko, 1983), and ABR thresholds almost reached the adult level by P14. In contrast, R75W+ mice have never showed ABR waveforms throughout postnatal development, indicating the disturbance of auditory organ development. The ABR thresholds in R75W+ mice exceeded 95 dB, which is comparable to profound deafness observed in human congenital deafness due to *GJB2* mutations.

Histological examinations of the cochleae with H-E staining revealed no obvious changes of Reissner's membrane, stria vascularis, spiral ligament, and spiral ganglion cells in the mutant mice (Fig. 2). On the other hand, a

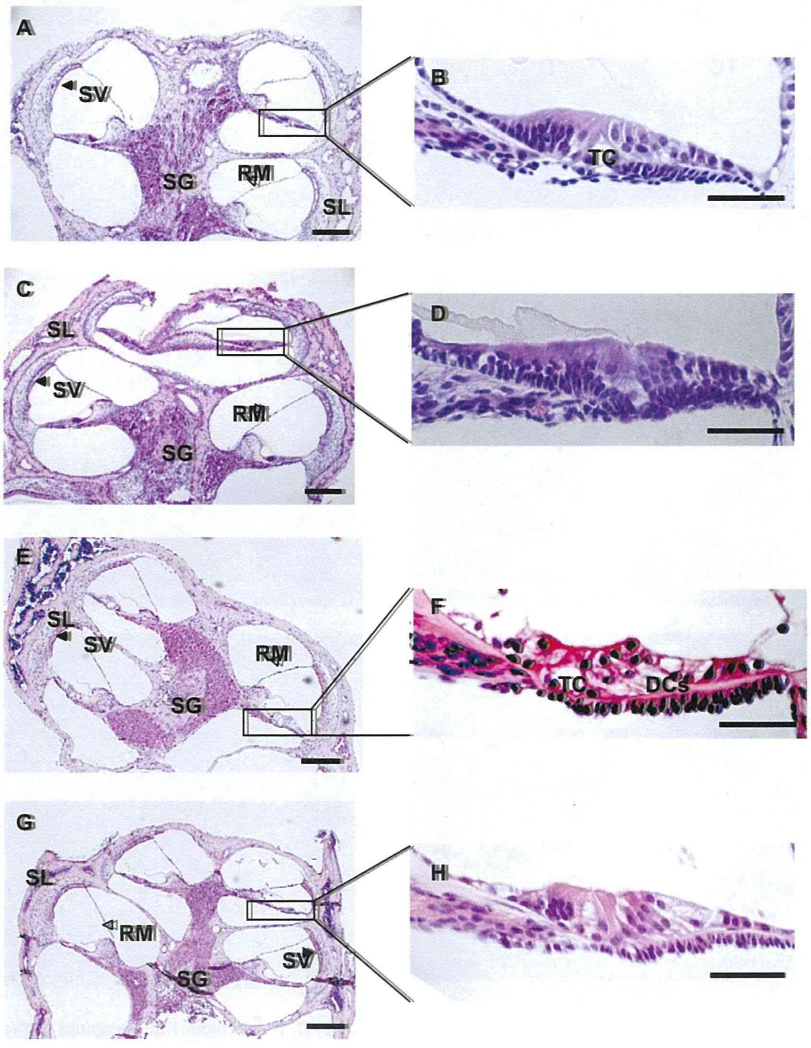

Fig. 2. Light microscopic findings of the cochlea. H-E staining presents defective changes in the organ of Corti obtained from animals at P8 (A, B) and P12 (E, F) of non-Tg mice and at P8 (C, D) and P12 (G, H) of R75W+ mice. Midmodiolar section was counterstained with H-E staining. No obvious changes are observed in RM; SV, SL, or SG (A, B, E, F). At P8 before the onset of hearing, tunnel of Corti is detected in non-Tg mice (B), but not in R75W+ mice (D). At P12, the DCs sit beneath the OHCs and Nuel's spaces are detected in non-Tg mice (F), but not in R75W+ mice (H). Abbreviations used: RM, Reissner's membrane; SV, stria vascularis; SL, spiral ligament; SG, spiral ganglion cells; TC, tunnel of Corti. Scale bar=100 μm (A–D); 50 μm (E–H).

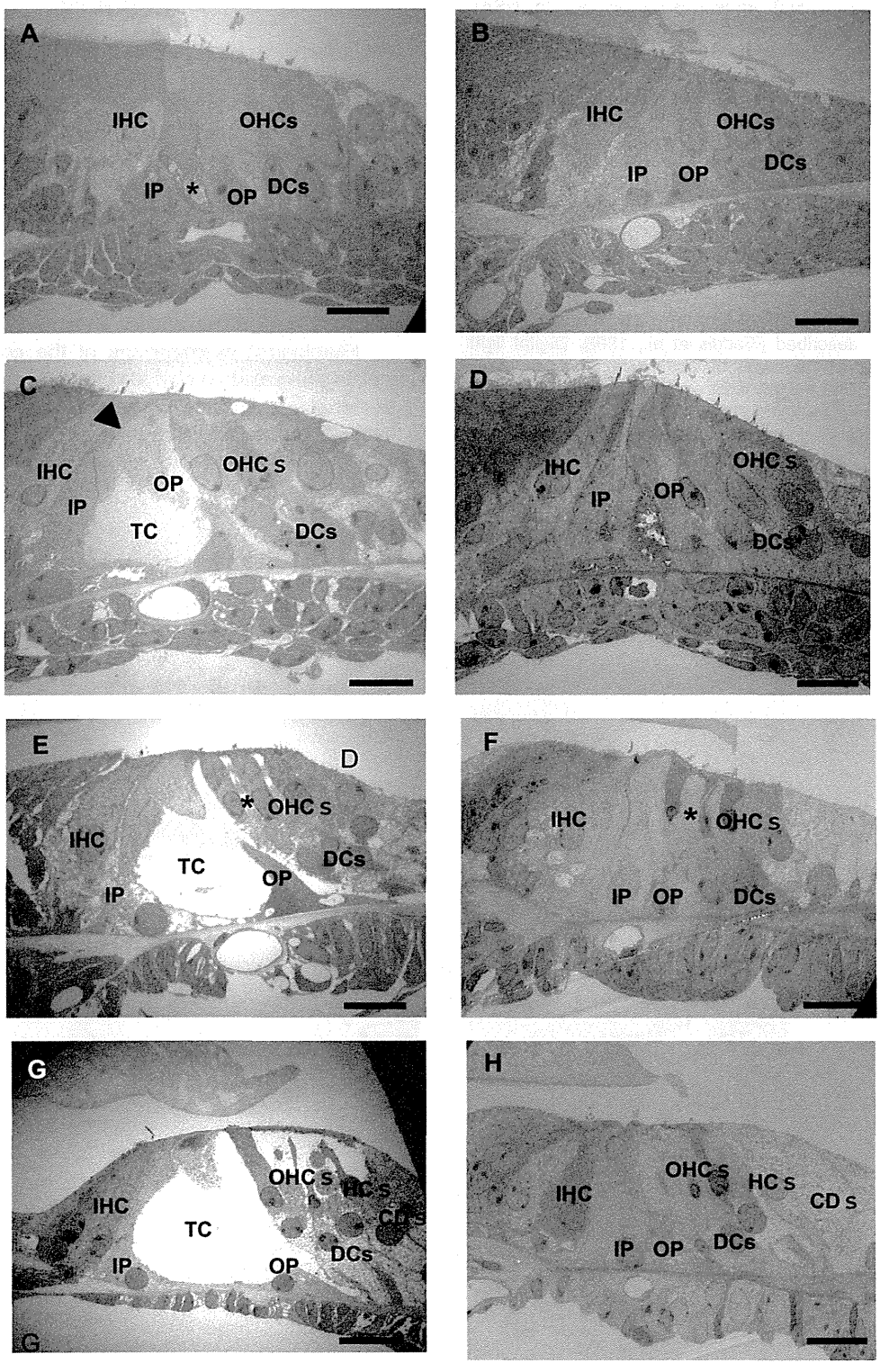

Fig. 3. Transmission electron micrographs of non-Tg (A, C, E, G) and R75W+ (B, D, F, H) mice. Future space of the tunnel of Corti (asterisk) starts to be formed in non-Tg mice (A), but is not detected in R75W+ mice (B) at P5. At P8, the open space between the IPCs and OPCs below their connection at a tight junction exceeds that of non-Tg mice (arrowhead in C). The TC is insufficient to be created in R75W+ mice (D). At P10, Nuel's space starts to be formed in non-Tg (asterisk in E) but not in R75W+ mice (asterisk in F). At P12, an adult-like configuration of the organ of Corti is created in non-Tg mice (G). The cell cytoplasm of supporting cells is enlarged in R75W+ mice (H). OHCs in R75W+ mice are squeezed by the surrounding DCs (F, H). Scale bar=10 μm. Abbreviations used: TC, tunnel of Corti; IP, inner pillar cell; OP, outer pillar cell; HC, Hensen cells; CDs, Claudius cells.

remarkable change of the collapse was recognized in the organ of Corti at least from P10 in the light microscopy (data not shown).

Ultrastructural analysis was performed to evaluate the fine structure of the organ of Corti in the late developmental stage. An analysis by TEM demonstrated further details of histological alterations in the organ of Corti (Fig. 3). The opening of tunnel of Corti between the IPC and outer pillar cell (OPC) were seen at P5 in non-Tg mice (Fig. 3A). In contrast, no spaces within IPC and OPC were apparent at P5 onward in R75W+ mice (Fig. 3B). No obvious structural change was observed in the other cells of the organ of Corti at P5. At P8 in both non-Tg and R75W+ mice, during expansion of tunnel of Corti, the pillar cell bodies were distinguished from the surrounding cells (Fig. 3C, D). At P10 in non-Tg mice, extensive Nuel's space opening occurred (Fig. 3E). In contrast, the future Nuel's spaces were occupied by bulky processes of Deiter's cells (DCs) in R75W+ mice (Fig. 3F). At P12, non-Tg mice approached a well-matured configuration (Fig. 3G). Supporting cells of R75W+ mice (Fig. 3H) tended to be grossly enlarged as compared with non-Tg. In the R75W+ mice, the IHC from P5 to P12 and the OHC from P5 to P8 had a relatively normal shape. Numerous mitochondria were located along the lateral membrane of the OHCs which was lined by a thick layer of subsurface cisternae (data not shown). However, DCs surrounded and compressed the OHCs at P10–12 (Fig. 3F, 3H).

Both IPCs and OPCs showed a nearly mature appearance, in which abundant microtubules were formed parallel array in non-Tg mice (Fig. 4A) whereas microtubules of the IPCs were poorly formed and hypoplasia occurred in R75W+ mice (Fig. 4B). Actually, the average number of microtubules of the cross-section of the IPCs at P12 in R75W+ mice (4.4±3.3/100 μm^2) was significantly reduced (Fig. 4D) as compared with that of non-Tg mice (26.9±25.6/100 μm^2) (Fig. 4C).

Quantitative data describing peak height and cell areas of the organ of Corti also showed the differences between non-Tg and R75W+ mice (Fig. 5). The height of the organ of Corti in non-Tg mice showed an increase with the development of the organ of Corti as described previously (Souter et al., 1997). In contrast, the height remained unchanged presumably due to collapse of tunnel of Corti in R75W+ mice (Fig. 5A). The cell area of the organ of Corti showed no difference between non-Tg and R75W+ mice at P5, both of which increased rapidly until P8. Although the increase of cell area appeared slowly after the formation of tunnel of Corti and Nuel's space at P8 in non-Tg mice, the area increased from P10 to P12 in R75W+ mice (Fig. 5B). The increase of the cell area from P10–12 recognized in R75W+ mice is assumed to be brought about by the enlarged supporting cells. Thus, the dominant-negative mutant of *Gjb2* disrupted postnatal development of supporting cells.

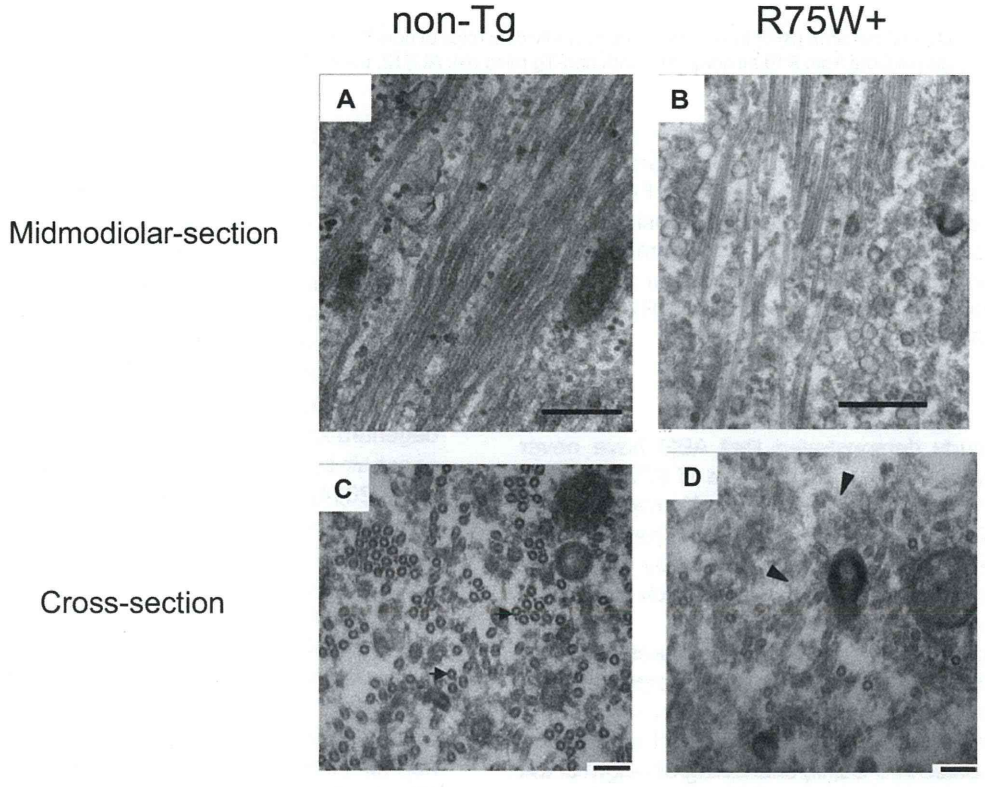

Fig. 4. The microtubules of the midmodiolar- (A, B) and cross-sections (C, D) of the IPC at P12. The microtubules are rich in the IPC in non-Tg mice (arrows in A). The microtubules of the IPC are poorly formed and hypoplasia in R75W+ mice (arrows in B). Round-shaped microtubules with cross-sections are abundant in non-Tg mice (arrows in C). (D) The number of microtubules is reduced and the tangled microtubules (arrows in D) are prominent in R75W+ mice. Scale bar=500 nm (A, B); 1 μm (C, D).

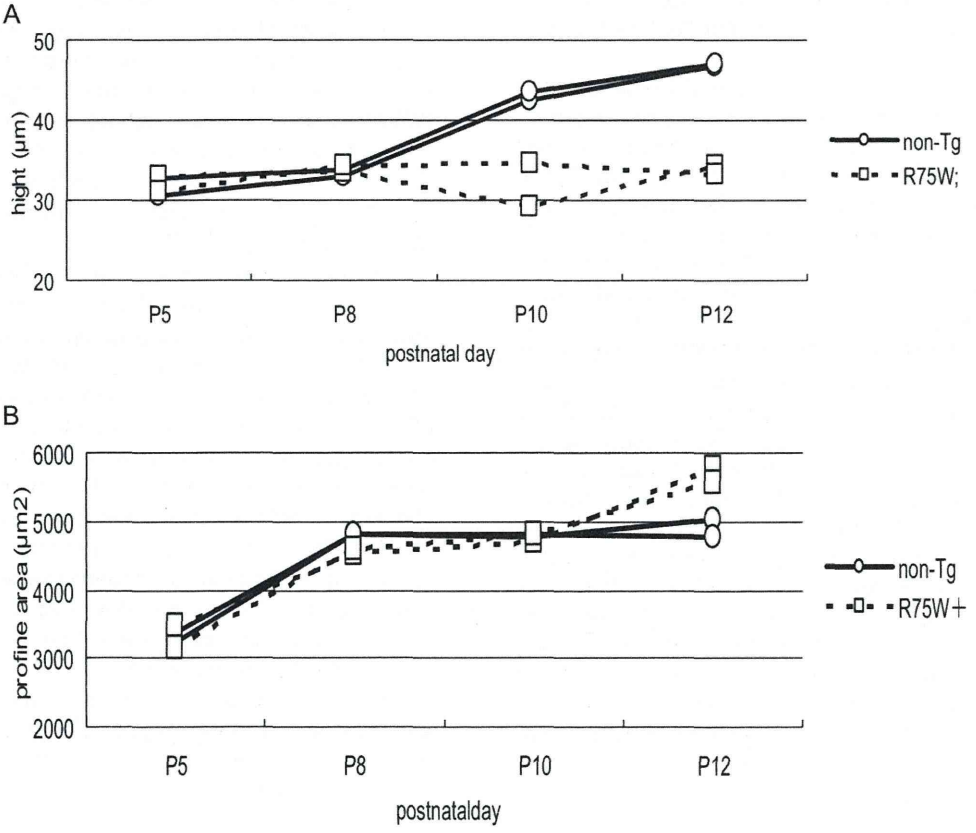

Fig. 5. The height of (A) and cell area (B) of the organ of Corti in individual mice of non-Tg (n=2) and R75W+ (n=2). R75W+ mice show the reduction of the height of the organ of Corti from P10 as compared with non-Tg mice (A). At P12, the profile area of the organ of Corti of R75W+ mice is greater than that of non-Tg mice (B).

Since it is possible that the *Gjb2* gene affects the known genes to determine or differentiate regarding hair or supporting cells, the protein expression of FGFR3 and $p27^{Kip1}$ for supporting cell markers, and MyosinVIIa for a hair cell marker were examined at P12. Similar results regarding the immunolabeling of the cochlear section for the tested antibodies were obtained in both R75W+ and non-Tg mice (Fig. 6).

DISCUSSION

The present study demonstrated that ABR have never been recognized in the postnatal stage of R75W+ mice from P5 to P14. On the other hand, non-Tg mice showed the onset of ABR at P11, which approached near maturity until P14. These findings may be explained by the supposition that the cochlear function does not reach maturation in a dominant-negative mutation of *Gjb2*.

The characteristic changes of ultrastructures observed in the developing non-sensory cells of the organ of Corti include: i) absence of tunnel of Corti, Nuel's space, or spaces surrounding the OHCs; ii) significant small numbers of microtubules in IPCs; iii) shortening of height of the organ of Corti; and iv) increase of the midmodiolar-sectional area of the cells of the organ of Corti. Thus, morphological observations confirmed that a dominant-negative *Gjb2* mutation showed incomplete development of the cochlear supporting cells. On the other hand, the development of the sensory hair cells at least from P5 to P12 was not affected, which is not surprising since the sensory hair cells do not express Cx26 throughout development. In fact, *MyosinVIIa*, a major gene identified in hair cells was expressed in the developing hair cells of R75W+ mice.

Our dominant-negative *Gjb2* mutant mice showed a phenotype apparently different from that of a target disruption of *Gjb2* (Cohen-Salmon et al., 2002), in which the inner ear normally developed up to P14 followed by the degeneration of the cochlear epithelial networks and sensory hair cells. Furthermore, our preliminary study (Ikeda et al., 2004) in a creation of a conditional knockout of *Gjb2* using the promoter different from that of Cohen-Salmon et al. (2002) showed comparable findings to the present dominant-negative *Gjb2* mutant. Both animal models of *Gjb2*-based hereditary deafness developed by us strongly indicate that *Gjb2* is indispensable throughout the postnatal development of the organ of Corti, especially from P5 to maturation.

The development of pillar cells and the formation of a normal tunnel of Corti are required for normal hearing (Colvin et al., 1996). The factors that regulate pillar cells development are *Fgfr3* (Mueller et al., 2002). The mice homozygous for a targeted disruption of *Fgfr3* had striking inner ear defects and were deaf. In the organ of Corti of

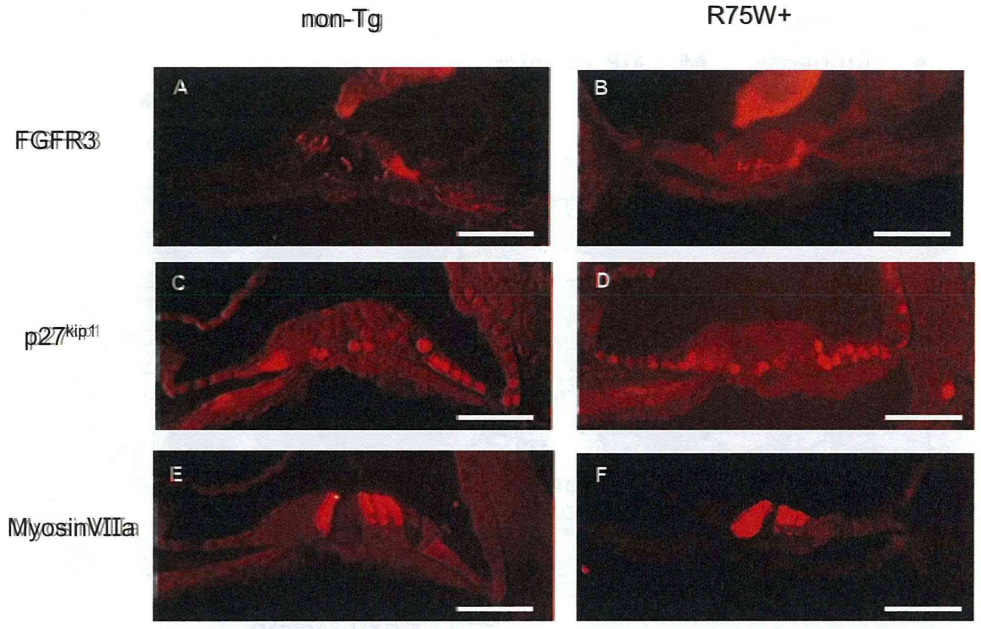

Fig. 6. Immunohistochemical analysis of the inner ear. Expressions of the FGFR3 are specifically localized in pillar cells in both non-Tg (A) and R75W+ (B). Expressions of the $p27^{Kip1}$ are labeled in nucleus of supporting cells in both non-Tg (C) and R75W+ (D). The inner and OHCs are labeled with MyosinVIIa in both non-Tg (E) and R75W+ (F). Scale bar=100 μm.

Fgfr3 deficient mice, differentiated pillar cells and the tunnel space were completely absent and ABR showed no response at 100 dB SPL (Colvin at al., 1996), which is interesting as it is similar to the observations of our R75W+ mice. It is possible that the cochlear *Gjb2* regulates differentiation genes of the supporting cells at the transcriptional or translational level. However, the expression of *Fgfr3* and $p27^{Kip1}$ proteins in the R75W+ mouse cochlea was equivalent to those of non-Tg mouse, which seems to negate the involvement of *Fgfr3* and $p27^{Kip1}$ genes to the disrupted differentiation of pillar cells and other supporting cells. It is possible to cause the effect similar to *Fgfr3* disruption by mediating its upstream and downstream pathways. Further studies are required to obtain a better understanding of the relevance of the *Fgfr3* pathway. The mutant mice of thyroid hormonal receptors were reported to have delayed postnatal development of the organ of Corti (Rusch et al., 2001). The phenotype of thyroid hormonal receptor mutants is similar to our phenotype with respect to the unopened tunnel of Corti, but not to the formation of tectorial membrane or the development of EP. Although the typical distribution of prestin along the OHC lateral membrane was found to depend on the thyroid hormone receptor TRβ (Winter et al., 2006), prestin was normally expressed in our Tg mice (our unpublished observations). These findings suggest that thyroid hormone is not related to the phenotype of the *Gjb2* dominant-negative mutation.

The results presented here demonstrate a significant reduction of the number of microtubules in the pillar cells in R75W+ mice, which presumably causes absence of the tunnel and incomplete height of the organ of Corti. The microtubules in the pillar cells appear to be unique to mammalian cochlea with respect to the aspect of a strong and rigid cytoskeleton for maintenance of cell shape and effective transduction of vibratory stimuli on the sensory epithelium (Saito and Hama, 1982; Slepecky et al., 1995). The disturbed formation of microtubules in DCs, which were not evaluated in the present study, is expected to take a place similar to pillar cells and may lead to failure to form Nuel's space as well as a lack of DC cup surrounding the hair cells and the nerve ending.

Morphometric analysis of cross-sectional areas of the cells of the organ of Corti suggests the reduction of cell volume whereas extracellular spaces such as tunnel of Corti, Nuel's space, and spaces surrounding OHCs were apparently diminished under the TEM observation. Inhibitory effects of channels, transporters, and fluid secretion are suspected to be mediated by cell-signal molecules through the gap junctions (Beltramello et al., 2005; Lang et al., 2007; Piazza et al., 2007; Zhang et al., 2005; Zhao et al., 2005). K-Cl cotransporters encoded by Kcc3 and Kcc4 are selectively expressed in DCs from late postnatal development and are thought to regulate the cell volume and the ionic environment of cortilymph (Boettger et al., 2002, 2003). The mouse cochlea deleting Kcc3 or Kcc4 resemble the phenotype of our R75W+ mice, implying that the increase of sectional-area of the cells of the organ of Corti may involve dysfunction of K-Cl cotransport in the DCs of R75W+ mice. The progressive degeneration of hair cells observed in the adult R75W+ mice (Kudo et al., 2003) may be brought about by the changes in the ionic composition of the cortilymph surrounding the basolateral surface of the hair cells (Ben-Yosef et al., 2003).

Gap junction proteins in the cochlear supporting cells are hypothesized to allow rapid removal of K^+ away from the base of hair cells, resulting in recycling back to the endolymph (Kikuchi et al., 1995). In addition to the K^+

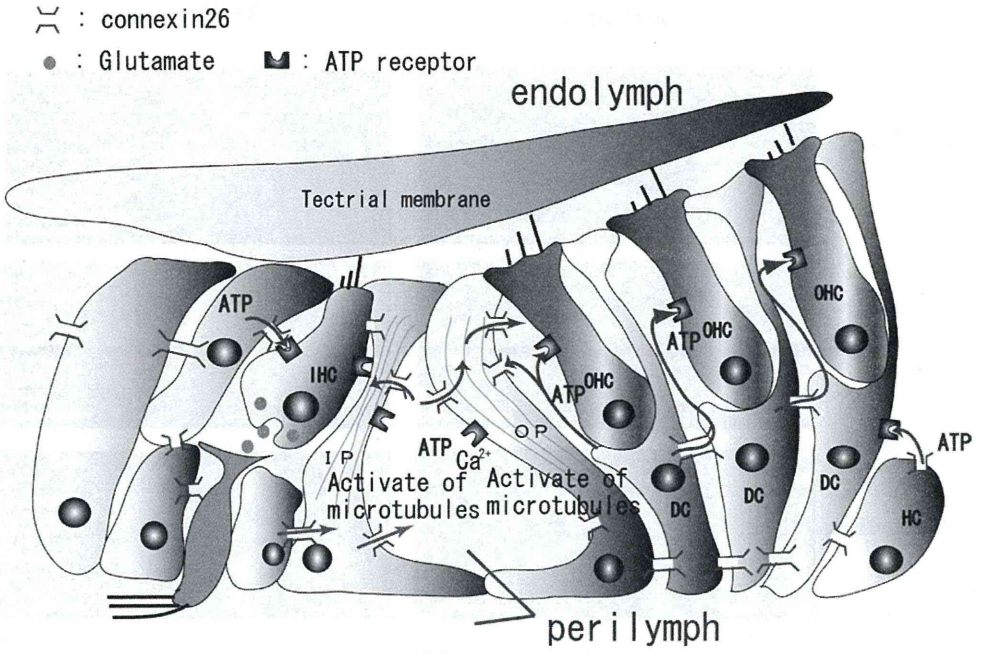

Fig. 7. Hypothesized schematic diagram of proposed intercellular signaling pathways between supporting cells and hair cells in the cochlea. ATP released from supporting cells via connexin hemichannels activates purinergic receptors on the hair cells or supporting cells in an autocrine and paracrine manner. Defective Cx26 is postulated to disrupt depolarization in the IHC and OHC, which may influence the glutamate release and the production of neurotrophic factors, respectively. Moreover, the failure of polymerization of the microtubules in the pillar cells may result from the disturbance of ATP release and/or intercellular signal transduction.

recycling theory, Ca^{2+} and anions such as inositol 1,4, 5-trisphosphate, ATP, and cAMP are mediated by gap junction proteins to act as cell-signaling and nutrient and energy molecules (Beltramello et al., 2005; Piazza et al., 2007; Zhang et al., 2005; Zhao et al., 2005). More currently, Tritsch et al. (2007) found that, in the postnatal immature cochlea, a transient structure known as Kölliker organ releases ATP through the hemichannels of its gap junctions, which binds to P2X receptors on the IHCs to cause depolarization and Ca^{2+} influx, mimicking the effect of sound. The resulting release of glutamate activates receptors on the afferent fibers, which is essential for the development of the auditory pathway. ATP is known to act as trophic factor, mitogen and potent neuromodulator (Fields and Burnstock, 2006; Nedergaard et al., 2003). Since supporting cells express ATP receptors (Dulon et al., 1993), the same scenario is likely to occur in an adapted form with the organ of Corti. The supporting cells may have an influence on maturation, cell volume and cell shape at least through the polymerization of microtubules by activated by ATP in an autocrine and paracrine manner (Zhao et al., 2005). We propose the hypothesis of an underlying mechanism to explain the prelingual deafness caused by *Gjb2* mutation (Fig. 7). Defective gap junction impairs the release of ATP and other factors related to cell-signaling and nutrient and energy molecules, resulting in the disturbance of normal postnatal development of the organ of Corti. Postnatal maturation of the various cochlear cells in the organ of Corti rapidly and synchronously progressed at P5 to P12 and may be regulated by intercellular signal transduction mediated by ions and biomodulators via the gap junction network derived from Cx26. Furthermore, a similar hypothesis may involve the postnatal development of the stria vascularis and spiral ligament because of the presence of purinergic receptors (Ikeda et al., 1995; Liu et al., 1995; Ogawa and Schacht, 1995) and the source of ATP (White et al., 1995; Suzuki et al., 1997).

CONCLUSION

In conclusion, the present findings strongly support that *Gjb2* is indispensable in the postnatal development of the organ of Corti and normal hearing.

Acknowledgments—This work was supported in part by research grant from the Ministry of Education, Science, and Culture of Japan (Nos. 16209050, 17659538, and 19659441) and Uehara Memorial Foundation.

REFERENCES

Anniko M (1983) Postnatal maturation of cochlear sensory hairs in the mouse. Anat Embyol (Berl) 166:355–368.

Beltramello M, Piazza V, Bukauskas FF, Pozzan T, Mammano F (2005) Impaired permeability to Ins(1,4,5)P3 in a mutant connexin underlies recessive hereditary deafness. Nat Cell Biol 2005 7:63–69.

Ben-Yosef T, Belyantseva IA, Saunders TL, Hughes ED, Kawamoto K, Van Itallie CM, Beyer LA, Halsey K, Gardner DJ, Wilcox ER, Rasmussen J, Anderson JM, Dolan DF, Forge A, Raphael Y, Camper SA, Friedman TB (2003) Claudin 14 knockout mice, a model for autosomal recessive deafness DFNB29, are deaf due to cochlear hair cell degeneration. Hum Mol Genet 12:2049–2061.

Boettger T, Hübner CA, Maier H, Rust MB, Beck FX, Jentsch TJ (2002) Deafness and renal tubular acidosis in mice lacking the K-Cl co-transporter Kcc4. Nature 416:874–878.

Boettger T, Rust MB, Maier H, Seidenbecher T, Schweizer M, Keating DJ, Faulhaber J, Ehmke H, Pfeffer C, Scheel O, Lemcke B, Horst J, Leuwer R, Pape HC, Völkl H, Hübner CA, Jentsch TJ (2003) Loss of K-Cl co-transporter KCC3 causes deafness, neurodegeneration and reduced seizure threshold. EMBO J 22:5422–5434.

Cohen-Salmon M, Ott T, Michel V, Hardelin JP, Perfettini I, Eybalin M, Wu T, Marcus DC, Wangemann P, Willecke K, Petit C (2002) Targeted ablation of connexin26 in the inner ear epithelial gap junction network causes hearing impairment and cell death. Curr Biol 12:1106–1111.

Colvin JS, Bohne BA, Harding GW, McEwen DG, Ornitz DM (1996) Skeletal overgrowth and deafness in mice lacking fibroblast growth factor receptor 3. Nat Genet 12:390–397.

Dulon D, Moataz R, Mollard P (1993) Characterization of Ca^{2+} signals generated by extracellular nucleotides in supporting cells of the organ of Corti. Cell Calcium 14:245–254.

Elias LA, Wang DD, Kriegstein AR (2007) Gap junction adhesion is necessary for radial migration in the neocortex. Nature 448: 901–907.

Faddis BT, Hughes RM, Miller JD (1998) Quantitative measures reflect degeneration, but not regeneration, in the deafness mouse organ of Corti. Hear Res 115:6–12.

Fields RD, Burnstock G (2006) Purinergic signaling in neuron-glia interactions. Nat Rev Neurosci 7:423–436.

Frenz CM, Van de Water TR (2000) Immunolocalization of connexin 26 in the developing mouse cochlea. Brain Res Rev 32:172–180.

Gabriel HD, Jung D, Butzler C, Temme A, Traub O, Winterhager E, Willecke K (1998) Transplacental uptake of glucose is decreased in embryonic lethal connexin26-deficient mice. J Cell Biol 140:1453–1461.

Ikeda K, Kudo T, Jin ZH, Gotoh S, Katori Y, Kikuchi T, Minowa O, Noda T (2004) Conditional gene targeting of *Gjb2* results in profound deafness due to maturation failure of the organ of Corti. 27th Midwinter research meeting, #762.

Ikeda K, Suzuki M, Furukawa M, Takasaka T (1995) Calcium mobilization and entry induced by extracellular ATP in the non-sensory epithelial cell of the cochlear lateral wall. Cell Calcium 18:89–99.

Kikuchi T, Kimura RS, Paul DL, Adams JC (1995) Gap junctions in the rat cochlea: immunohistochemical and ultrastructural analysis. Anat Embryol 191:101–118.

Kudo T, Kure S, Ikeda K, Xia AP, Katori Y, Suzuki M, Kojima K, Ichinohe A, Suzuki Y, Aoki Y, Kobayashi T, Matsubara Y (2003) Transgenic expression of a dominant-negative connexin26 causes degeneration of the organ of Corti and non-syndromic deafness. Hum Mol Genet 12:995–1004.

Lang F, Vallon V, Knipper M, Wangemann P (2007) Functional significance of channels and transporters expressed in the inner ear and kidney. Am J Physiol Cell Physiol 293:C1187–C1208.

Liu J, Kozakura K, Marcus DC (1995) Evidence for purinergic receptors in vestibular dark cell and strial marginal cell epithelia of the gerbil. Auditory Neurosci 1:331–340.

Mueller KL, Jacques BE, Kelly MW (2002) Fibroblast growth factor signaling regulates pillar cell development in the organ of. Corti J Neurosci 22:9368–9377.

Nedergaard M, Ransom B, Goldman SA (2003) New roles for astrocytes: redefining the functional architecture of the brain. Trends Neurosci 26:523–530.

Ogawa K, Schacht J (1995) P2y purinergic receptors coupled to phosphoinositide hydrolysis in tissues of the cochlear lateral wall. Neurorepor 6:1538–1540.

Piazza V, Ciubotaru CD, Gale JE, Mammano F (2007) Purinergic signalling and intercellular Ca^{2+} wave propagation in the organ of Corti. Cell Calcium 41:77–86.

Rusch A, Ng L, Goodyear R, Oliver D, Lisoukov I, Vennstrom B, Richardson G, Kelley MW, Forrest D (2001) Retardation of cochlear maturation and impaired hair cell function caused by deletion of all known thyroid hormone receptors. J Neurosci 21:9792–9800.

Saito K, Hama K (1982) Structural diversity of microtubules in the supporting cells of the sensory epithelium of guinea pig organ of Corti. J Electron Microsc 31:278–281.

Slepecky NB, Henderson CG, Saha C (1995) Post-translational modifications of tubulin suggest that dynamic microtubules are present in sensory cells and stable microtubules are present in supporting cells of the mammalian cochlea. Hear Res 91:136–147.

Souter M, Nevill G, Forge A (1997) Postnatal maturation of the organ of Corti in gerbils: morphology and physiological responses. J Comp Neurol 386:635–651.

Suzuki H, Ikeda K, Furukawa M, Takasaka T (1997) P2 purinoceptor of the globular substance in the otoconial membrane of the guinea pig inner ear. Am J Physiol 273:C1533–C1540.

Tritsch NX, Yi E, Gale JE, Glowatzki E, Bergles DE (2007) The origin of spontaneous activity in the developing auditory system. Nature 450:50–55.

White PN, Thorne PR, Housley GD, Mockett B, Billett TE, Burnstock G (1995) Quinacrine staining of marginal cells in the stria vascularis of the guinea-pig cochlea: a possible source of extracellular ATP? Hear Res 90:97–105.

Winter H, Braig C, Zimmermann U, Geisler HS, Fränzer JT, Weber T, Ley M, Engel J, Knirsch M, Bauer K, Christ S, Walsh EJ, McGee J, Köpschall I, Rohbock K, Knipper M (2006) Thyroid hormone receptors TRalpha1 and TRbeta differentially regulate gene expression of Kcnq4 and prestin during final differentiation of outer hair cells. J Cell Sci 119:2975–2984.

Zhang Y, Tang W, Ahmad S, Sipp JA, Chen P, Lin X (2005) Gap junction-mediated intercellular biochemical coupling in cochlear supporting cells is required for normal cochlear function. Proc Natl Acad Sci U S A 102:15201–15206.

Zhao HB, Yu N, Fleming CR (2005) Gap junctional hemichannel-mediated ATP release and hearing controls in the inner ear. Proc Natl Acad Sci U S A 102:18724–18729.

(Accepted 11 August 2008)
(Available online 22 August 2008)

HUMAN GENE THERAPY 19:384–390 (April 2008)

DOI: 10.1089/hum.2007.167

Brief Report

Noninvasive *In Vivo* Delivery of Transgene via Adeno-Associated Virus into Supporting Cells of the Neonatal Mouse Cochlea

TAKASHI IIZUKA,[1] SHO KANZAKI,[2] HIDEKI MOCHIZUKI,[3] AYAKO INOSHITA,[1] YUYA NARUI,[1] MASAYUKI FURUKAWA,[1] TAKESHI KUSUNOKI,[1] MAKOTO SAJI,[4] KAORU OGAWA,[2] and KATSUHISA IKEDA[1]

ABSTRACT

There are a number of genetic diseases that affect the cochlea early in life, which require normal gene transfer in the early developmental stage to prevent deafness. The delivery of adenovirus (AdV) and adeno-associated virus (AAV) was investigated to elucidate the efficiency and cellular specificity of transgene expression in the neonatal mouse cochlea. The extent of AdV transfection is comparable to that obtained with adult mice. AAV-directed gene transfer after injection into the scala media through a cochleostomy showed transgene expression in the supporting cells, inner hair cells (IHCs), and lateral wall with resulting hearing loss. On the other hand, gene expression was observed in Deiters cells, IHCs, and lateral wall without hearing loss after the application of AAV into the scala tympani through the round window. These findings indicate that injection of AAV into the scala tympani of the neonatal mouse cochlea therefore has the potential to efficiently and noninvasively introduce transgenes to the cochlear supporting cells, and this modality is thus considered to be a promising strategy to prevent hereditary prelingual deafness.

INTRODUCTION

SEVERAL TYPES OF HEREDITARY DEAFNESS in humans have been matched with homologous mouse models (Eisen and Ryugo, 2007). Mice present an ideal model for inner ear gene therapy because their genome is being rapidly sequenced and their generation time is relatively short. To achieve effective gene therapy in hereditary deafness, it may be required to transfer corrective genes into the defective cochlear cells of neonatal mice. However, the small size of the neonatal mouse inner ear poses a particular challenge for performing surgical procedures.

Transgene expression has been successfully demonstrated in the mammalian inner ear, using various viral vectors including adenoviral (AdV) vectors (Raphael *et al.*, 1996), adeno-associated viral (AAV) vectors (Lalwani *et al.*,1996), herpes simplex viral vectors (Derby *et al.*, 1999), lentiviral vectors (Han *et al.*, 1999), and Sendai viral vectors (Kanzaki *et al.*, 2007). In this study, we tested AAV vectors and AdV vectors because AAVs are free of genotoxicity and present no evidence of pathogenicity in humans, and AdVs have high transfection efficiency in many tissues and cell types. In previous studies, the three main routes of delivery of viral vectors into the cochlea of the adult mouse, namely, the scala media approach, the semicircular canal approach, and the round window (RW) approach, have been reported (Kawamoto *et al.*, 2001; Suzuki *et al.*, 2003). The semicircular canal method was not used in this study because of its poor transduction of genes.

The present study assessed how to inject a gene into the neonatal mouse cochlea on postnatal day 0 (P0); the results indicate that this modality is a promising therapeutic strategy to prevent prelingual deafness.

[1]Department of Otorhinolaryngology, Juntendo University School of Medicine, Tokyo 113-8421, Japan.
[2]Department of Otolaryngology, Keio University, Tokyo 160-0016, Japan.
[3]Department of Neurology, Juntendo University School of Medicine, Tokyo 113-8421, Japan.
[4]Department of Physiology, School of Allied Health Sciences, Kitasato University, Sagamihara 228-8555, Japan.

MATERIALS AND METHODS

Animals

Twenty healthy C57BL/6 mouse pups, irrespective of gender, were used on P0 (within 24 hr of birth). All experimental protocols were approved by the Institutional Animal Care and Use Committee at Juntendo University (Tokyo, Japan), and were conducted in accordance with the U.S. National Institutes of Health *Guide for the Care and Use of Laboratory Animals.*

Adenoviral and adeno-associated viral vectors

A replication-deficient adenoviral vector (human AdV, serotype 5) was used to encode the green fluorescent protein (GFP) driven by the cytomegalovirus (CMV) promoter. The virus was designated Ad5.CMV-GFP (3×10^{11} plaque-forming units [PFU]/ml). The E1 and E3 regions were deleted. Vectors were purchased from Primmune KK (Osaka, Japan). Viral suspensions in 10 m*M* Tris-HCl (pH 7.5), 1 m*M* $MgCl_2$, and 10% glycerol were kept at –80°C until thawed for use.

The plasmid DNA pAAV-MCS (CMV promoter; Stratagene, La Jolla, CA) carrying the GFP gene was constructed as reported previously (Yamada *et al.*, 2004). The plasmid DNA pAAV-GFP was cotransfected with plasmids pHelper and Pack2/1 into HEK-293 cells, using the standard calcium phosphate method (Sambrook and Russell, 2001). After 48 hr, cells were harvested and crude recombinant AAV (rAAV) vector (serotype 1) solutions were obtained by repeated freeze–thaw cycles. After ammonium sulfate precipitation, the viral particles were dissolved in phosphate-buffered saline (PBS) and applied to an OptiSeal centrifugation tube (Beckman Coulter, Fullerton, CA). After overlaying OptiPrep solution (Axis-Shield PoC, Oslo, Norway), the tube was processed with a Gradient Master (BioComp Instruments, Fredericton, NB, Canada) to prepare a gradient layer of OptiPrep. The tube was then ultracentrifuged at 13,000 rpm for 18.5 hr. The fractions containing high-titer rAAV vectors were collected and used for injection into animals. The number of rAAV genome copies was semiquantified by polymerase chain reaction (PCR) within the CMV promoter region using primers 5′-GACGTCAATAATGACGTATG-3′ and 5′-GGTAATAGCGATGACTAATACG-3′. The final titer was 1.4×10^{13} viral particles (VP)/ml.

Surgical procedures

Glass capillaries (Drummond Scientific, Broomall, PA) were drawn with a PB-7 pipette puller (Narishige, Tokyo, Japan) to achieve an approximately 10-μm outer tip diameter. A polyethylene tube (outer diameter, 1.7 mm; Atom Medical, Saitama, Japan) was connected to the glass micropipette.

For injection into the scala media via a cochleostomy, C57BL/6 mice were anesthetized with ketamine (100 mg/kg) and xylazine (4 mg/kg) by intraperitoneal injection. A left postauricular incision was made and the otic bulla was exposed, and opened to expose the cochlea. A cochleostomy was made at the cochlear lateral wall of a basal turn just beneath the stapedial artery with the glass micropipette, using a micromanipulator. The bony lateral wall of the cochlea on P0 is so soft that it can be easily penetrated by the glass micropipette. The injection volume of the viral vector was regulated at approximately 0.02 μl/min for 10 min, using a syringe connected to the polyethylene tube. To allow the vector to spread throughout and stabilize in the inner ear, the glass micropipette was left in place for 1 min after the injection. The hole was plugged and the opening in the tympanic bulla was sealed with connective tissue. The total surgical period was approximately 20 min.

For injection into the scala tympani after anesthesia, the otic bulla was opened to expose the RW. Next, the glass micropipette was inserted into the RW (Fig. 1), and the vectors were injected in the same manner as in the scala media approach. Because the hole in the RW membrane was extremely small, leakage of perilymph was found to be nominal after re-

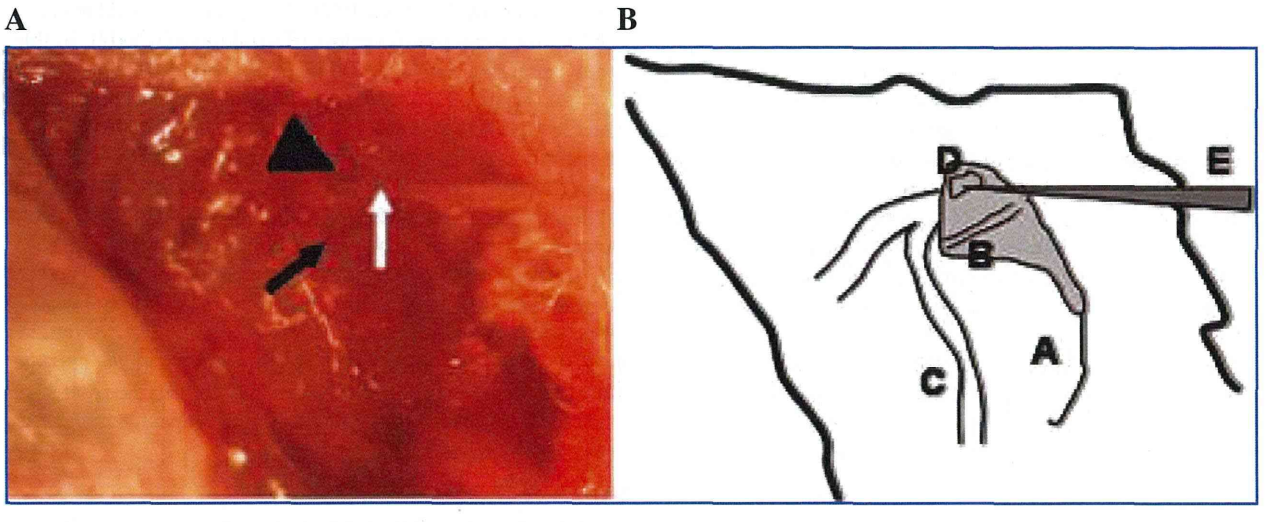

FIG. 1. Surgical procedure for microinjection into the neonatal mouse cochlea. The otic bulla was exposed after a left postauricular incision. The otic bulla is transparent. After opening the otic bulla, a round window (arrowhead) and the stapedial artery (solid arrow) are seen. Viral vectors were injected into the scala tympani with a glass micropipette (open arrow) inserted into the RW membrane. A, tympanic bulla; B, stapedial artery; C, facial nerve; D, round window; E, glass micropipette.

moving the micropipette. It took approximately 20 min to complete the surgical procedure. After the surgery, the mice were kept in another cage until they awoke from anesthesia.

Measurements of auditory brainstem response

To determine the surgical effects on auditory function, the auditory brainstem response (ABR) were assessed 14 days postoperatively. Hearing thresholds were determined in both ears: the injected side (left) and the contralateral noninjected control side (right). ABR measurements were performed as previously reported (Kanzaki *et al.*, 2007). Thresholds were determined for frequencies of 4, 8, 12, 16, and 20 kHz from a set of responses at various intensities with 5-dB intervals and electrical signals were averaged at 512 repetitions. If the hearing threshold was over 95 dB, then it was determined to be 100 dB.

Sample preparation, histology, and immunohistochemical analysis

On day 14 after injection, the mice were deeply anesthetized and perfused intracardially with PBS, followed by 4% paraformaldehyde in phosphate buffer. The cochleae were excised and then tissue specimens were fixed in 4% paraformaldehyde for 2 hr and decalcified in 0.12 *M* EDTA for 7 days at room temperature. For frozen sections, specimens were cryoprotected in 30% sucrose in PBS overnight at 4°C, and then were embedded, frozen, and sectioned at 10 μm. For immunofluorescence, sections were incubated with 50% Block Ace (AbD Serotec/MorphoSys, Martinsried, Germany) in PBS–0.3% Triton X-100 for 60 min and then they were incubated overnight at 4°C with goat polyclonal anti-GFP antibodies (diluted 1:200 in PBS; Santa Cruz Biotechnology, Santa Cruz, CA). The next day, tissue specimens were rinsed with PBS, incubated for 60 min with rabbit anti-goat IgG antibodies conjugated with Alexa Fluor 488 (diluted 1:500; Invitrogen Molecular Probes, Eugene, OR), and rinsed with PBS. Subsequently, all specimens were incubated with rhodamine phalloidin (diluted 1:100; Invitrogen Molecular Probes) for 30 min and then were mounted in VECTASHIELD antifade mounting medium with 4′,6-diamidino-2-phenylindole (DAPI; Vector Laboratories, Burlingame, CA).

Images of sections were captured with a Zeiss Axioplan 2 microscope (Carl Zeiss, Oberkochen, Germany), using an AxioCam HRc charge-coupled device (CCD) camera and the AxioVision release 4.5 software program.

Data analysis

The KaleidaGraph statistical software program (Synergy Software, Reading, PA) was used for the statistical analysis of the ABR data.

RESULTS

All of the animals recovered uneventfully from surgery and survived until ABR measurements were performed. No signs of vestibular disturbance, such as circling behavior or head tilting, were observed.

After the injection of AdV vectors into the scala media (n = 3), GFP-positive cells were present mainly in the supporting cells (Fig. 2A), mesothelial cells of the scala tympani and scala vestibuli, and cells of Reissner's membrane. Injection of AdV through the RW (n = 5) induced the expression of GFP only in the mesothelial cells lining the perilymphatic spaces (Fig. 2B). No GFP-positive cells were found in either the organ of Corti or the lateral wall. GFP expression was identified in various cochlear cells (Fig. 2C), predominantly in both the inner hair cells and the supporting cells of the organ of Corti after AAV injection into the scala media (n = 6), and the loss of hair cells, as noted in a previous report (Ishimoto *et al.*, 2002), was not observed in these mice (Fig. 2D). Application of AAV to the scala tympani across the RW (n = 6) showed that GFP-positive cells were found mainly in the supporting cells (Fig. 2E), and loss of hair cells was not (Fig. 2F). These results are summarized in Table 1. An examination of the contralateral (right) ears of AAV injected mice revealed a normal appearance with no pathological hair cell loss, and no GFP-positive cells were seen (Fig. 2G and H).

Before killing the mice on P14, ABR thresholds were assessed in both ears, on both the injected side and contralateral side. In the groups injected with AAV (Fig. 3A) or AdV vectors (Fig. 3B) by the scala tympani approach through the RW, the ABR thresholds did not differ significantly from those of contralateral noninjected control sides at any frequency tested. On the other hand, a significant threshold shift at each frequency was seen in the group injected with either AAV (Fig. 3C) or AdV vectors (Fig. 3D) by the scala media approach via cochleostomy, in comparison with those on the contralateral control sides.

DISCUSSION

To our knowledge this is the first report demonstrating successful gene delivery to the neonatal mouse cochlea *in vivo*. It is ideal to transfer a normal gene noninvasively to a hereditary deafness mouse model at an early time after birth, before differentiation of the cochlear sensory structures. The procedure of gene delivery to the animal models must yield efficient gene transduction without hearing loss.

Excellent gene expression without hearing loss was obtained by selecting both the appropriate application route (the

FIG. 2. Sagittal cryosections of the mouse cochlea. GFP-expressing cells (green) are seen by fluorescence microscopy in cochlear sagittal cryosections of P14 mice that had been injected on P0. Rhodamine phalloidin antibody was used as a marker for hair cells (red). (**A**) Cochlear section after exposure to AdV by scala media injection. Transduced Deiters cells and outer pillar cells (arrows) expressed GFP. (**B**) After exposure to AdV by scala tympani injection. Only mesothelial cells of the perilymph expressed GFP. GFP were absent in the organ of Corti. (**C** and **D**) Cochlear section after exposure to AAV by scala media injection. (**C**) Transduced supporting cells (Deiters cells, Hensen cells, and Claudius cells; arrowheads) expressed GFP. (**D**) No loss of hair cells was observed with the nuclear label DAPI (blue). (**E** and **F**) After exposure to AAV by scala tympani injection, transduced Deiters cells (arrows) expressed GFP (**E**), and loss of hair cells was not observed (**F**). (**G** and **H**) Cochlear section of contralateral (right) ears after exposure to AAV by both scala media injection (**G**) and scala tympani injection (**H**) revealed a normal appearance with no pathological hair cell loss, and no GFP-positive cells were seen. Scale bar in (**A**) (for **A**–**H**): 100 μm.